mater.scichina.com link.springer.com

Published online 6 May 2023 | https://doi.org/10.1007/s40843-022-2422-3
*Sci China Mater* 2023, 66(7): 2822–2828

# Pressure-induced superconductivity in topological heterostructure $(PbSe)_5(Bi_2Se_3)_6$

Cuiying Pei[1†], Peng Zhu[2,3,4†], Bingtan Li[5,6], Yi Zhao[1], Lingling Gao[1], Changhua Li[1], Shihao Zhu[1], Qinghua Zhang[7], Tianping Ying[7], Lin Gu[7], Bo Gao[8], Huiyang Gou[8], Yansun Yao[9], Jian Sun[10], Hanyu Liu[5,6], Yulin Chen[1,11,12], Zhiwei Wang[2,3,4*], Yugui Yao[2,3] and Yanpeng Qi[1,11,13*]

**ABSTRACT** **Recently, the natural heterostructure of $(PbSe)_5(Bi_2Se_3)_6$ has been theoretically predicted and experimentally confirmed as a topological insulator. In this work, we induce superconductivity in $(PbSe)_5(Bi_2Se_3)_6$ by implementing high pressures. As the pressure increases up to 10 GPa, superconductivity with a critical temperature ($T_c$) ~ 4.6 K suddenly appears, which is followed by an abrupt decrease. Remarkably, upon further compression above 30 GPa, a new superconducting state arises, where pressure raises the $T_c$ to an unsaturated 6.0 K within the limit of our research. Combining X-ray diffraction and Raman spectroscopy, we suggest that the emergence of the two distinct superconducting states occurs concurrently with the pressure-induced structural transition in this topological heterostructure $(PbSe)_5(Bi_2Se_3)_6$.**

**Keywords:** high pressure, superconductivity, heterostructure, topological material

## INTRODUCTION

Heterostructures are layered structures that contain an interface between different materials, which is often advantageous to engineer the electronic energy bands in many solid-state device applications, including semiconductor lasers, solar cells, and transistors [1–8]. Fabrication of heterostructures has long been limited by deposition or epitaxial techniques, e.g., molecular beam epitaxy (MBE) and metalorganic chemical vapor deposition (MOCVD), hindering extensive studies of the unique material systems. Hence, natural multilayer heterostructures with homogeneous interfaces are desired and can provide new opportunities to study the novel physical properties.

The Pb-based homologous series of $(PbSe)_5(Bi_2Se_3)_{3m}$ ($m$ = 1, 2), one of the natural multilayer heterostructures, has recently attracted attention [9–13]. The structure is generally regarded as an alternating layered structure of $m$ quintuple layers (QLs) of $Bi_2Se_3$ with bilayer PbSe, and it is naturally formed as a multilayer heterostructure. Because the binary compound $Bi_2Se_3$ is well known to be a topological insulator (TI) [14,15] and PbSe is a topologically trivial one [16], $(PbSe)_5(Bi_2Se_3)_{3m}$ ($m$ = 1, 2) consists of ultrathin TI layers separated by trivial-insulator layers. Interestingly, Nakayama *et al.* [11] observed gapped Dirac-cone dispersions with a large band gap of 0.5 eV for $m$ = 2 *via* angle-resolved photoemission spectroscopy (ARPES), showing that topological interface states are effectively encapsulated by the PbSe block layers. Such a multilayer system with topological and ordinary insulating layers is an interesting playground for realizing novel topology.

Recently, unconventional superconductivity has been reported experimentally in $(PbSe)_5(Bi_2Se_3)_{3m}$ ($m$ = 1, 2) by Cu intercalations and Ag doping, offering a potential platform to observe the Majorana fermion state at the boundary of natural heterostructures [13,17,18]. Pressure is an effective method to tune the lattice structure and to manipulate the electronic state without introducing impurities. It has been shown that the pressure can induce superconductivity in topological phases of matter [19–22]. In this work, we report two distinct pressure-induced

[1] School of Physical Science and Technology, ShanghaiTech University, Shanghai 201210, China
[2] Centre for Quantum Physics, Key Laboratory of Advanced Optoelectronic Quantum Architecture and Measurement (MOE), School of Physics, Beijing Institute of Technology, Beijing 100081, China
[3] Beijing Key Lab of Nanophotonics and Ultrafine Optoelectronic Systems, Beijing Institute of Technology, Beijing 100081, China
[4] Material Science Center, Yangtze Delta Region Academy of Beijing Institute of Technology, Jiaxing 314011, China
[5] State Key Laboratory of Superhard Materials and International Center for Computational Method and Software, College of Physics, Jilin University, Changchun 130012, China
[6] International Center of Future Science, Jilin University, Changchun 130012, China
[7] Beijing National Laboratory for Condensed Matter Physics, Institute of Physics, Chinese Academy of Sciences, Beijing 100190, China
[8] Center for High Pressure Science and Technology Advanced Research, Beijing 100094, China
[9] Department of Physics and Engineering Physics, University of Saskatchewan, Saskatoon, Saskatchewan S7N 5E2, Canada
[10] National Laboratory of Solid State Microstructures, School of Physics and Collaborative Innovation Center of Advanced Microstructures, Nanjing University, Nanjing 210093, China
[11] ShanghaiTech Laboratory for Topological Physics, ShanghaiTech University, Shanghai 201210, China
[12] Department of Physics, Clarendon Laboratory, University of Oxford, Parks Road, Oxford OX1 3PU, UK
[13] Shanghai Key Laboratory of High-resolution Electron Microscopy, ShanghaiTech University, Shanghai 201210, China
[†] These authors contributed equally to this work.
[*] Corresponding authors (emails: qiyp@shanghaitech.edu.cn (Qi Y); zhiweiwang@bit.edu.cn (Wang Z))

  

superconducting states in the topological heterostructure $(PbSe)_5(Bi_2Se_3)_6$. Under high pressures, superconductivity with a critical temperature ($T_c$) ~ 4.6 K suddenly appears at around 10 GPa and is then suppressed abruptly, forming a superconducting state (SC-I) in the pressure-temperature phase diagram. Another superconducting state (SC-II) emerges above 30 GPa, of which the $T_c$ increases slowly upon compression and a maximum and unsaturated $T_c$ of 6.0 K is obtained within the limit of our research. The two distinct pressure-induced superconducting states in the topological heterostructure $(PbSe)_5(Bi_2Se_3)_6$ is accompanied by a structural transition, as evidenced by both the X-ray diffraction (XRD) and Raman data.

## EXPERIMENTAL SECTION

### Materials

High-quality single crystals of $(PbSe)_5(Bi_2Se_3)_6$ were grown by using a combination of a melting method and the modified Bridgman method [23]. High-purity starting materials of Bi, Pb, and Se were loaded in a quartz tube with the ratio of $PbSe:Bi_2Se_3$ = 38:62. The tube was sealed after it was evacuated to a vacuum of $2 \times 10^{-4}$ Pa. The raw materials reacted and were homogenized at 1173 K for several hours, and then the crystal growth was fostered by slowly cooling down the temperature from 983 to 913 K in 560 h in a temperature gradient of roughly 1 K $cm^{-1}$. Then the grown rod was fast-cooled to room temperature. In order to obtain crystals with high quality, we performed surface cleaning for all starting materials to remove the oxide layers formed in the air [24,25].

### Characterization of materials in ambient pressure

The scanning transmission electron microscopy (STEM) measurements were performed on a high-quality $(PbSe)_5(Bi_2Se_3)_6$ single crystal. After the single crystal was fully ground in acetone, the small fragments suspended in acetone were dripped onto a TEM microgrid. The atomic positions of $(PbSe)_5(Bi_2Se_3)_6$ were characterized using an ARM-200CF (JEOL, Tokyo, Japan) transmission electron microscope operated at 200 kV. The XRD measurements were performed on a Bruker AXS D8 Advance powder crystal X-ray diffractometer with Cu Kα1 ($\lambda$ = 1.54178 Å) at room temperature.

### Electricity transport measurements under high pressures

High-pressure electric resistivity measurements of $(PbSe)_5(Bi_2Se_3)_6$ crystals were performed by the van der Pauw four-probe method with NaCl as the pressure transmitting medium (PTM) as described elsewhere [22,26,27]. A cubic BN/epoxy mixture was used as an insulation layer. Platinum leads were arranged in nonmagnetic copper beryllium (BeCu) diamond anvil cells. The pressure was calibrated by the ruby measurements at room temperature [28]. A magnet-cryostat (Dynacool, Quantum Design, $T_{min}$ = 1.8 K) was used to take the cryogenic setup and magnetic field measurements.

### Raman measurements under high pressures

High-pressure *in-situ* Raman spectroscopy investigation on $(PbSe)_5(Bi_2Se_3)_6$ was carried out on a Raman spectrometer (Renishaw in Via, U.K.) with a laser excitation wavelength of 532 nm as well as a low-wavenumber filter. Symmetric diamond anvil cell (DAC) with anvil culet sizes of 300 μm and mineral oil was used as the PTM. The pressure was calibrated by the ruby measurements at room temperature [28].

### Synchrotron XRD measurements under high pressures

The pressure dependence of the XRD pattern was measured at beamline 15U at Shanghai Synchrotron Radiation Facility (X-ray wavelength $\lambda$ = 0.6199 Å). Symmetric DAC with anvil culet sizes of 300 μm and T301 gaskets were used. Neon and mineral oil were used as the PTM, and the pressure was determined by the ruby luminescence method [28]. Rietveld refinements of the crystal structures under high pressures were performed using the general structure analysis system (GSAS) and graphical user interface EXPGUI package [29].

## RESULTS AND DISCUSSION

$(PbSe)_5(Bi_2Se_3)_6$ crystallizes in a monoclinic structure $C2/m$ (No. 12). Prior to high-pressure measurements, we first checked the sample quality by single-crystal XRD diffractions and STEM, as shown in Fig. 1 and Fig. S1. The single-crystal XRD data reveal that the ($h$00) plane is a natural cleavage facet of as-grown single crystals. The extracted lattice parameters are $a$ = 50.3858 Å, in agreement with a previous report [30]. An annular dark-field STEM (ADF-STEM) image of $(PbSe)_5(Bi_2Se_3)_6$ along [010] is shown in Fig. 1b. Bi atoms are located at the centre of distorted Se octahedra, while Pb atoms are surrounded by Se atoms and form a distorted polyhedron. An alternate stack of $Bi_2Se_3$ and PbSe along the $a$ axis builds a multilayer heterostructure in a monoclinic unit cell belonging to the space group of $C2/m$. An interesting observation is that one slice of the PbSe layer drifts 1/10 off the $c$-axis (highlighted in the red solid and broken parallelograms). These atomic drifts within one unit cell cannot be reflected in our powder XRD patterns, but they are prevalent in all the observed ADF-STEM images. Such dislocations should be an inherent property of this misfit layered compound, introducing significant strain and distortion to alter its physical properties. The above characterizations indicate the high quality of our samples.

Fig. 2 shows the evolution of temperature dependence of the electrical resistivity of $(PbSe)_5(Bi_2Se_3)_6$ for pressures up to 73.2 GPa. At 0.6 GPa, the resistivity of $(PbSe)_5(Bi_2Se_3)_6$ in the whole pressure range shows a metallic-like nature with residual resistivity ratio (RRR) of 2.53. In the low-pressure region, increasing pressure initially induces a continuous enhancement of the overall magnitude of $\rho$, with a maximum occurring at around 10 GPa. Then the resistivity decreases slowly. Meanwhile, a superconducting transition where resistivity reaches zero emerges at 4.6 K suddenly. Subsequently, the superconducting transition temperature $T_c^{onset}$ is suppressed to a minimum of 1.9 K at around 25–30 GPa. Surprisingly, $T_c^{onset}$ starts to increase rapidly with further increase in pressure above 32 GPa, reaching a value of 6.0 K at 37.5 GPa. So, a pressure-induced reentrant superconducting state was observed for $(PbSe)_5(Bi_2Se_3)_6$. With the pressure further increasing, $T_c^{onset}$ increases slowly to an unsaturated $T_c$ of 6.2 K obtained within the limit of our research.

There are two distinct pressure-induced superconducting regions. To further identify the difference between these two superconducting states, we applied magnetic fields on $(PbSe)_5(Bi_2Se_3)_6$ subjected to 11.6 and 47.0 GPa, respectively. As shown in Fig. 2d, the zero-resistance state at 11.6 GPa is continuously suppressed by the magnetic field until it vanishes over 3.0 T. On

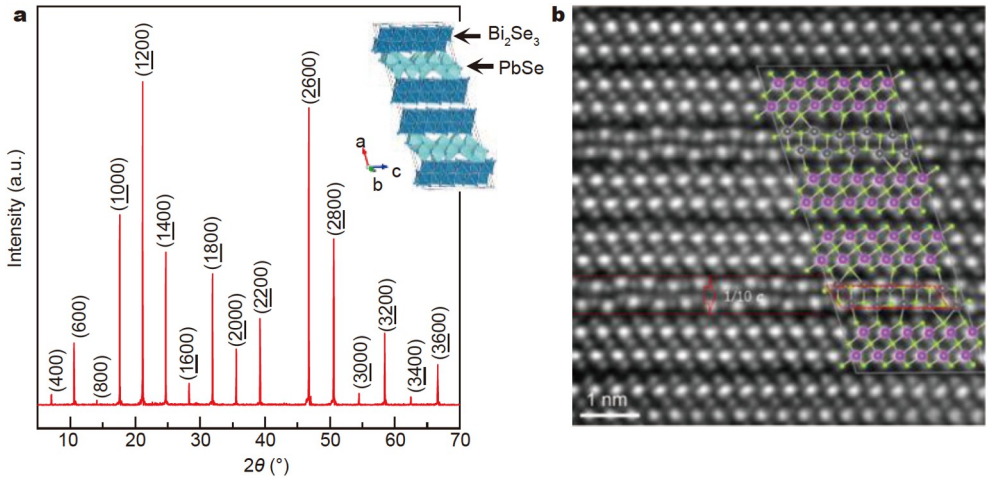


**Figure 1** (a) XRD pattern of $(PbSe)_5(Bi_2Se_3)_6$ single crystal at ambient pressure. Inset: crystal structure of $(PbSe)_5(Bi_2Se_3)_6$. (b) Angular dark-field (ADF) image of $(PbSe)_5(Bi_2Se_3)_6$. Their respective crystal structures are superimposed. Aberration-corrected STEM image of $(PbSe)_5(Bi_2Se_3)_6$ with well-organized atomic position along [010]. The crystal structures given in the inorganic crystal structure database (ICSD) are superimposed for comparison. Solid and broken parallelograms highlight the supposed and actual atomic position of the PbSe layer, respectively. The red broken lines isolate the PbSe layer that drifts along the *a*-axis by 1/10.

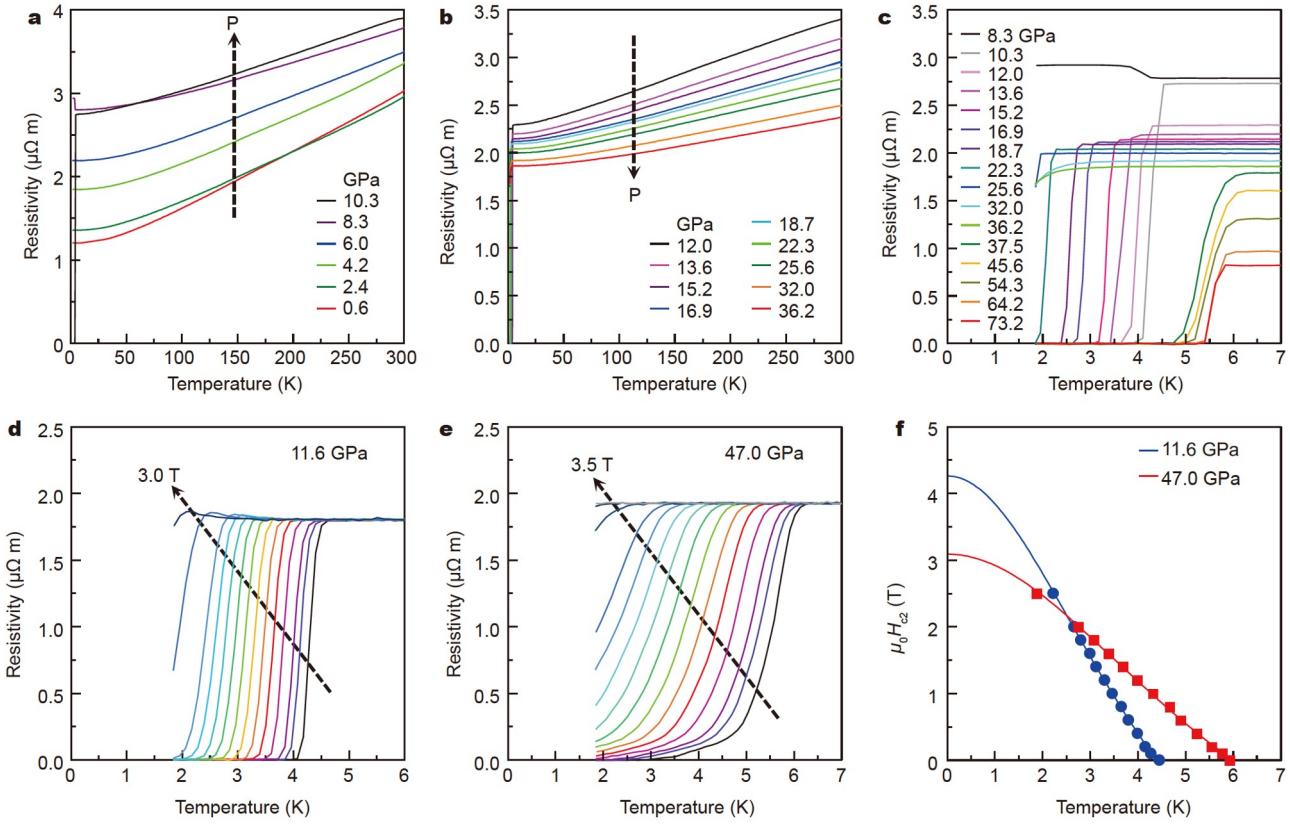


**Figure 2** Transport properties of $(PbSe)_5(Bi_2Se_3)_6$ as a function of pressure. Electrical resistivity as a function of temperature for pressures of 0.6–10.3 GPa (a) and 12.0–36.2 GPa (b). (c) Temperature-dependent resistivity of $(PbSe)_5(Bi_2Se_3)_6$ in the vicinity of the superconducting transition. Temperature dependence of resistivity under different magnetic fields for $(PbSe)_5(Bi_2Se_3)_6$ at 11.6 GPa (d) and 47.0 GPa (e). (f) Temperature dependence of upper critical field $\mu_0 H_{c2}(T)$ at 11.6 and 47.0 GPa. Here, the $T_c$ values are determined at 90% of the normal state resistivity just above the onset superconducting transition temperature. The solid dots and squares stand for the temperature dependence of resistivity under different magnetic fields for $(PbSe)_5(Bi_2Se_3)_6$ at 11.6 and 47.0 GPa, respectively. The solid lines represent the fits using the Ginzburg-Landau formula.

application of the magnetic field to the compressed sample at 47.0 GPa, similar behavior was observed (Fig. 2e). These results confirm that the resistivity drop in both two superconducting states is related to superconducting transition. Fig. 2f shows the Ginzburg-Landau fitting ($H_{c2}(T) = H_{c2}(0)\frac{1-t^2}{1+t^2}$, where $t = T/T_c$ is

  

thenormalized temperature) on the field dependence of $T_c$ for $(PbSe)_5(Bi_2Se_3)_6$ at 11.6 and 47.0 GPa, respectively [27,31,32]. The estimated critical fields $\mu_0 H_{c2}(0) \approx 4.3$ and 3.1 T for 11.6 and 47.0 GPa, respectively. Although the $\mu_0 H_{c2}$ obtained here is lower than its corresponding Pauli paramagnetic limit $H_P = 1.84T_c$, the slopes of $dH_{c2}/dT$ are notably different: −1.16 and −0.63 T K$^{-1}$ for 11.6 and 47.0 GPa, respectively. Our results demonstrate distinct different nature between the two pressure-induced superconducting states. Using the relation of $\xi_{GL}(0) = \sqrt{\phi_0 / 2\pi\mu_0 H_{c2}(0)}$, where $\phi_0$ is the flux quantum, we derive G-L coherence length $\xi_{GL}(0)$ 9.8 nm at 11.6 GPa and 10.3 nm at 47.0 GPa, respectively. The details are summarized in Table 1.

To investigate whether the observed two distinct superconducting states in pressurized $(PbSe)_5(Bi_2Se_3)_6$ are associated with a pressure-induced crystal structure phase transition, we performed *in situ* high-pressure XRD measurements. The XRD patterns of $(PbSe)_5(Bi_2Se_3)_6$ collected at different pressures are shown in Fig. 3a. A representative refinement at 0.5 GPa is displayed in Fig. S2. All the diffraction peaks can be indexed well to the ambient monoclinic structure with a space group of $C2/m$ (No. 12). Using the ideal hydrostaticity Ne as the PTM, the ambient phase is robust and can remain till 9.4 GPa. Above that, several peaks are involved which are attributed to a new high-pressure phase (Phase II). This phase is stable in a pressure range of 10.3–23.9 GPa. Above 28.4 GPa, Phase III was observed and coexisted with Phase II upon compression (Figs S3–S5). We could not get pure Phase III even at the pressure of 61.0 GPa. It should be noted that structure searches for this system by CALYPSO or other methods failed because of its complicated atom configuration [33–35]. To derive more structural phase transition information, high-pressure *in-situ* Raman spectroscopy measurement was carried out on $(PbSe)_5(Bi_2Se_3)_6$. As shown in Fig. 3b, all four phonon modes show a blue shift arising from an enhancement of the van der Walls forces between adjacent layers with pressure increasing. An abrupt disappearance of Raman modes at 11.6 GPa indicates pressure-induced structural phase transition, which is consistent with our synchrotron XRD patterns. In summary, our *in-situ* XRD and Raman spectroscopy measurements demonstrate that two distinct high-pressure phases were achieved in $(PbSe)_5(Bi_2Se_3)_6$ upon compression.

The pressure-dependent $T_c$ and related physical parameters are summarized in Fig. 4. To confirm the emergence of the two distinct superconducting states under high pressures, we repeated the measurements with new samples for several runs and proved that all the results are reproducible (Figs S6–S11). The *P*-$T_c$ phase diagram reveals three different regions: the initial non-superconducting Phase I (around 0–10 GPa) and the pressure-induced superconducting Phase II (10–30 GPa) and Phase III (30–80 GPa). For the normal state, we fit the $\rho(T)$ curve by the equation of $\rho = \rho_0 + AT^n$ from $T_c$ to 70 K, where $\rho_0$ is the residual resistivity, $n$ is the temperature exponent, and $A$ is a constant. The pressure-dependent key transport parameters are also plotted in Fig. 4. In Phase I, $\rho_0$ increases with pressure while $n$ maintains around 2, showing a Fermi-liquid behavior [36]. No superconductivity was observed down to 1.8 K in this pressure range. In Phase II, a superconducting transition with $T_c \sim 4.6$ K suddenly appears accompanied by a first structural phase transition. However, $T_c$ is sensitive to pressure and decreases sharply upon compression. Only a small drop without zero resistivity was observed at a pressure of around 30 GPa. Meanwhile, $A$ quickly decreases from 0.25 to 0.01 nΩ m K$^{-2}$, and $n$ increases from 1.5 to 2.0, implying that the electron-correlated states possibly transit from non-Fermi-liquid to Fermi-liquid state. In Phase III, a new superconducting phase suddenly emerges after

**Table 1** A summary of superconductivity properties of $(PbSe)_5(Bi_2Se_3)_6$ under high pressures

| Phase | $T_c$ (K) | $H_{c2}(0)$ (T) | $dH_{c2}/dT$ (T K$^{-1}$) | $\xi_{GL}(0)$ (nm) |
|---|---|---|---|---|
| SC-I (11.6 GPa) | 4.6 | 4.3 | −1.16 | 9.8 |
| SC-II (47.0 GPa) | 6.0 | 3.1 | −0.63 | 10.3 |

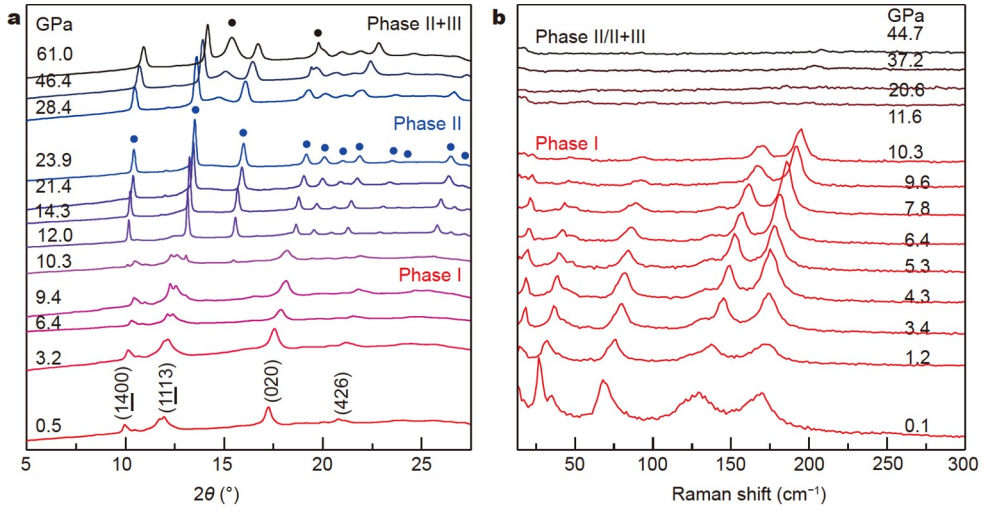


**Figure 3** Pressure dependence of XRD patterns (a) and Raman spectra (b) at room temperature of $(PbSe)_5(Bi_2Se_3)_6$, respectively. High-pressure *in-situ* synchrotron XRD was measured at Shanghai Synchrotron Radiation Facility with X-ray wave-length $\lambda = 0.6199$ Å.

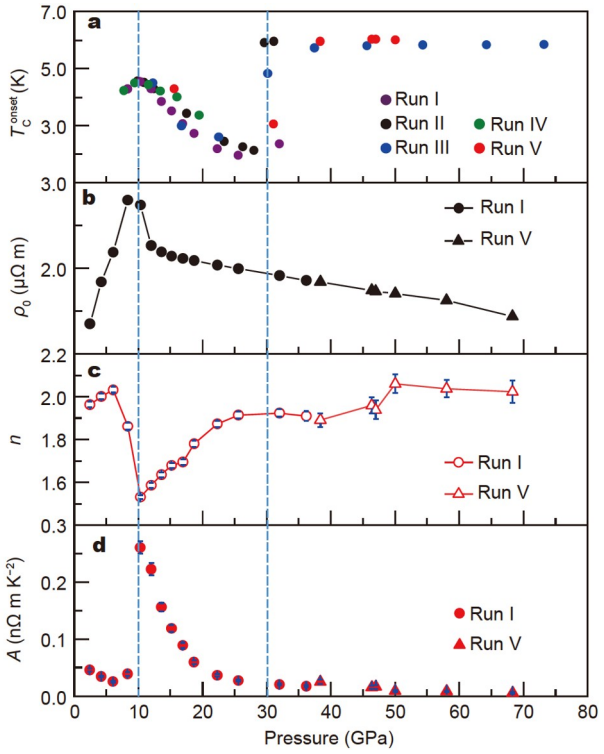


**Figure 4** The temperature-pressure diagram of $(PbSe)_5(Bi_2Se_3)_6$. (a) Pressure-dependent $T_c$ of $(PbSe)_5(Bi_2Se_3)_6$. The red, olive, blue, purple, and black solid circles represent the $T_c$ extracted from different runs of resistivity measurements. Pressure-dependent residual resistivity $\rho_0$ (b), temperature exponent $n$ (c), and constant $A$ (d) of $(PbSe)_5(Bi_2Se_3)_6$.

the second structural phase transition, showing pressure-induced reemergence of superconductivity. $T_c$ was enhanced as high as 6 K, which is higher than that in Phase II. Upon further increasing the pressure, $T_c$ increases slowly without saturation in our measured pressure limit. At this stage, $A$ does not change so much and $n$ keeps at around 2, which is similar to the initial phase.

Finally, we would like to compare the high-pressure effect between the multilayer heterostructure and building blocks (PbSe and $Bi_2Se_3$). First, pressure-induced multi-phase transitions were observed in heterostructure $(PbSe)_5(Bi_2Se_3)_6$ and its individual building blocks (PbSe and $Bi_2Se_3$). For PbSe, it undergoes a structural phase transition from NaCl- (Phase I) to GeS-type lattice (Phase II) at 2–6 GPa with resistivity abruptly rising [37–39]. In further compression above 15 GPa, another structural phase transition to a CsCl-type structure (Phase III) occurs, accompanied by a semiconductor–metal conversion. For $Bi_2Se_3$, a pressure-induced structural phase transition occurs from ambient rhombohedra structure (Phase I, $R\bar{3}m$) to monoclinic structure (Phase II, $C2/m$) at ~10 GPa and to body-centered tetragonal structure (Phase III, $I4/mmm$) at ~25 GPa [14,15]. Second, the application of pressure effectively tuned the electronic properties, and superconductivity was induced in both heterostructure $(PbSe)_5(Bi_2Se_3)_6$ and its building blocks (PbSe and $Bi_2Se_3$). For PbSe, superconductivity was only observed in Phase III (~30 GPa) with $T_c$ of 6.5 K [40]. Correspondingly, $Bi_2Se_3$ becomes superconducting at around 12 GPa with $T_c$ of 4.4 K [41]. With pressure increasing, $T_c$ increases to a maximum of 8.2 K at 17 GPa and then decreases to 6.5 K at 23 GPa [42]. Alternating layers of rocksalt PbSe and $Bi_2Se_3$ present diverse symmetry and periodicity, which results in an incommensurate structure. Fig. 5 summarizes the coevolution of crystal structures and $T_c$ under external pressure in $(PbSe)_5(Bi_2Se_3)_6$, PbSe, and $Bi_2Se_3$ for comparison. It is reasonable to predict the first superconducting dome given the onset of superconductivity in both PbSe and $Bi_2Se_3$ at moderate pressures. However, the reentrant of the second superconducting dome at phase III is quite unexpected. Such an emergent phenomenon might result from the interfacial effect of the infinite PbSe-$Bi_2Se_3$ stacking sequence. Further research is highly desired with the primary goal of determining its high-pressure structure in Phase III.

## CONCLUSIONS

In conclusion, we systematically investigated the electrical transport, structural, and lattice dynamical properties of the topological heterostructure $(PbSe)_5(Bi_2Se_3)_6$ under high pressures up to 80 GPa. Application of pressure effectively tuned the electronic properties and crystal structure of $(PbSe)_5(Bi_2Se_3)_6$. Two pressure-induced superconducting states are observed upon compression, which is related to a structural transition as

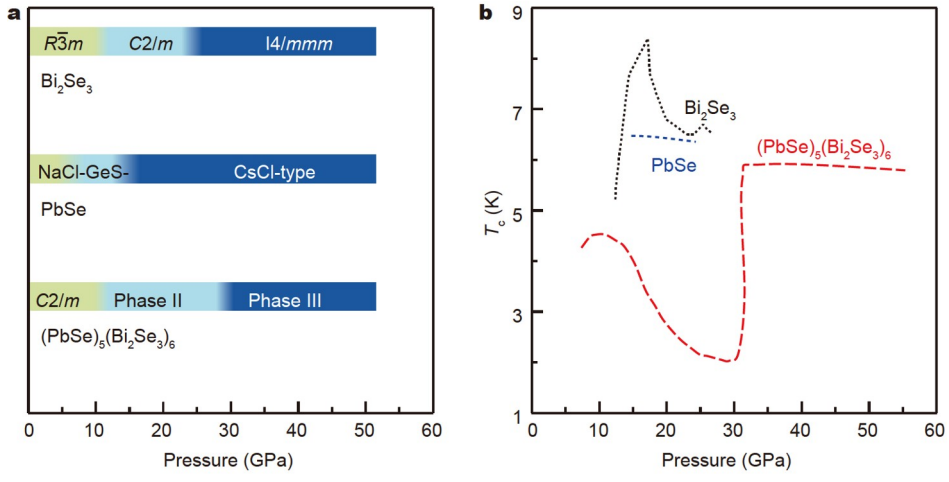


**Figure 5** Evolution of crystal structure (a) and superconductivity (b) of heterostructure $(PbSe)_5(Bi_2Se_3)_6$ and its building blocks (PbSe and $Bi_2Se_3$) under external pressures [14,15,37–42].

evidenced by both the XRD and Raman measurements. Besides natural multilayer heterostructure and nontrivial topology, our results demonstrate that $(PbSe)_5(Bi_2Se_3)_6$ exhibits new ground states upon compression.

**Received 17 December 2022; accepted 6 February 2023; published online 6 May 2023**


1 Serlin M, Tschirhart CL, Polshyn H, *et al.* Intrinsic quantized anomalous Hall effect in a Moiré heterostructure. Science, 2020, 367: 900–903
2 Buzdin AI. Proximity effects in superconductor-ferromagnet heterostructures. Rev Mod Phys, 2005, 77: 935–976
3 Žutić I, Fabian J, Das Sarma S. Spintronics: Fundamentals and applications. Rev Mod Phys, 2004, 76: 323–410
4 Barati F, Grossnickle M, Su S, *et al.* Hot carrier-enhanced interlayer electron-hole pair multiplication in 2D semiconductor heterostructure photocells. Nat Nanotech, 2017, 12: 1134–1139
5 Hyun WJ, Thomas CM, Luu NS, *et al.* Layered heterostructure ionogel electrolytes for high-performance solid-state lithium-ion batteries. Adv Mater, 2021, 33: 2007864
6 Yang X, Wang M, Li Y, *et al.* Superconductivity in a misfit compound $(PbSe)_{1.12}(TaSe_2)$. Supercond Sci Technol, 2018, 31: 125010
7 Bai H, Yang X, Liu Y, *et al.* Superconductivity in a misfit layered compound $(SnSe)_{1.16}(NbSe_2)$. J Phys-Condens Matter, 2018, 30: 355701
8 Pei C, Xia Y, Wu J, *et al.* Pressure-induced topological and structural phase transitions in an antiferromagnetic topological insulator. Chin Phys Lett, 2020, 37: 066401
9 Sassi S, Candolfi C, Delaizir G, *et al.* Crystal structure and transport properties of the homologous compounds $(PbSe)_5(Bi_2Se_3)_{3m}$ ($m$ = 2, 3). Inorg Chem, 2018, 57: 422–434
10 Sassi S, Candolfi C, Dauscher A, *et al.* Inelastic neutron scattering study of the lattice dynamics of the homologous compounds $(PbSe)_5(Bi_2Se_3)_{3m}$ ($m$ = 1, 2 and 3). Phys Chem Chem Phys, 2018, 20: 14597–14607
11 Nakayama K, Eto K, Tanaka Y, *et al.* Manipulation of topological states and the bulk band gap using natural heterostructures of a topological insulator. Phys Rev Lett, 2012, 109: 236804
12 Shelimova LE, Karpinskii OG, Zemskov VS. X-ray diffraction study of ternary layered compounds in the PbSe-$Bi_2Se_3$ system. Inorg Mater, 2008, 44: 927–931
13 Fang L, Stoumpos CC, Jia Y, *et al.* Dirac fermions and superconductivity in the homologous structures $(Ag_xPb_{1-x}Se)_5(Bi_2Se_3)_{3m}$ ($m$ = 1, 2). Phys Rev B, 2014, 90: 020504
14 Zhang H, Liu CX, Qi XL, *et al.* Topological insulators in $Bi_2Se_3$, $Bi_2Te_3$ and $Sb_2Te_3$ with a single Dirac cone on the surface. Nat Phys, 2009, 5: 438–442
15 Xia Y, Qian D, Hsieh D, *et al.* Observation of a large-gap topological-insulator class with a single Dirac cone on the surface. Nat Phys, 2009, 5: 398–402
16 Wrasse EO, Schmidt TM. Prediction of two-dimensional topological crystalline insulator in PbSe monolayer. Nano Lett, 2014, 14: 5717–5720
17 Nakayama K, Kimizuka H, Tanaka Y, *et al.* Observation of two-dimensional bulk electronic states in the superconducting topological insulator heterostructure $Cu_x(PbSe)_5(Bi_2Se_3)_6$: Implications for unconventional superconductivity. Phys Rev B, 2015, 92: 100508
18 Andersen L, Wang Z, Lorenz T, *et al.* Nematic superconductivity in $Cu_{1.5}(PbSe)_5(Bi_2Se_3)_6$. Phys Rev B, 2018, 98: 220512
19 Pei C, Zhang J, Wang Q, *et al.* Pressure-induced superconductivity at 32 K in $MoB_2$. Natl Sci Rev, 2023, 10: nwad034
20 Pei C, Huang P, Zhu P, *et al.* Pressure-induced superconductivity extending across the topological phase transition in thallium-based topological materials. Cell Rep Phys Sci, 2022, 3: 101094
21 Pei C, Xi M, Wang Q, *et al.* Pressure-induced superconductivity in magnetic topological insulator candidate $MnSb_4Te_7$. Phys Rev Mater, 2022, 6: L101801
22 Pei C, Ying T, Zhao Y, *et al.* Pressure-induced reemergence of superconductivity in $BaIr_2Ge_7$ and $Ba_3Ir_4Ge_{16}$ with cage structures. Matter Radiat at Extremes, 2022, 7: 038404
23 Segawa K, Taskin AA, Ando Y. $Pb_5Bi_{24}Se_{41}$: A new member of the homologous series forming topological insulator heterostructures. J Solid State Chem, 2015, 221: 196–201
24 Wang Z, Segawa K, Sasaki S, *et al.* Ferromagnetism in Cr-doped topological insulator $TlSbTe_2$. APL Mater, 2015, 3: 083302
25 Wang Z, Taskin AA, Frölich T, *et al.* Superconductivity in $Tl_{0.6}Bi_2Te_3$ derived from a topological insulator. Chem Mater, 2016, 28: 779–784
26 Pei C, Zhang J, Gong C, *et al.* Distinct superconducting behaviors of pressurized $WB_2$ and $ReB_2$ with different local B layers. Sci China-Phys Mech Astron, 2022, 65: 287412
27 Pei C, Ying T, Zhang Q, *et al.* Caging-pnictogen-induced superconductivity in skutterudites $IrX_3$ (X = As, P). J Am Chem Soc, 2022, 144: 6208–6214
28 Mao HK, Xu J, Bell PM. Calibration of the ruby pressure gauge to 800 kbar under quasi-hydrostatic conditions. J Geophys Res, 1986, 91: 4673–4676
29 Larson AC, Dreele RBV. General structure analysis system (GSAS). Los Alamos: Los Alamos National Laboratory Report LAUR, 2004. 86–748
30 Sasaki S, Segawa K, Ando Y. Superconductor derived from a topological insulator heterostructure. Phys Rev B, 2014, 90: 220504
31 Jones CK, Hulm JK, Chandrasekhar BS. Upper critical field of solid solution alloys of the transition elements. Rev Mod Phys, 1964, 36: 74–76
32 Woollam JA, Somoano RB, O'Connor P. Positive curvature of the $H_{c2}$-versus-$T_c$ boundaries in layered superconductors. Phys Rev Lett, 1974, 32: 712–714
33 Gao B, Gao P, Lu S, *et al.* Interface structure prediction *via* CALYPSO method. Sci Bull, 2019, 64: 301–309
34 Wang Y, Lv J, Zhu L, *et al.* Crystal structure prediction *via* particle-swarm optimization. Phys Rev B, 2010, 82: 094116
35 Wang Y, Lv J, Zhu L, *et al.* CALYPSO: A method for crystal structure prediction. Comput Phys Commun, 2012, 183: 2063–2070
36 Löhneysen H, Rosch A, Vojta M, *et al.* Fermi-liquid instabilities at magnetic quantum phase transitions. Rev Mod Phys, 2007, 79: 1015–1075
37 Ovsyannikov SV, Shchennikov VV, Popova SV, *et al.* Semiconductor-metal transitions in lead chalcogenides at high pressure. Phys Stat Sol (B), 2003, 235: 521–525
38 Shchennikov VV, Ovsyannikov SV, Derevskov AY. Thermopower of lead chalcogenides at high pressures. Phys Solid State, 2002, 44: 1845–1849
39 Ovsyannikov SV, Shchennikov VV, Manakov AY, *et al.* Unusual B1-B2 transition in PbSe under high pressure: Evidence for two intermediate phases; transport, structural, and optical properties. Phys Stat Sol (B), 2009, 246: 615–621
40 Brandt NB, Gitsu DV, Popovich NS. Superconductivity of the compounds PbTe and PbSe under high pressure. JETP Lett, 1975, 22: 104–105
41 Yu Z, Wang L, Hu Q, *et al.* Structural phase transitions in $Bi_2Se_3$ under high pressure. Sci Rep, 2015, 5: 15939
42 Kong PP, Zhang JL, Zhang SJ, *et al.* Superconductivity of the topological insulator $Bi_2Se_3$ at high pressure. J Phys-Condens Matter, 2013, 25: 362204


**Acknowledgements** This work was supported by the National Natural Science Foundation of China (12004252, 52272265, U1932217, 11974246, 52072400, 52025025, and 92065109), the National Key R&D Program of China (2018YFA0704300, 2021YFA1401800, 2018YFE0202601, 2020YFA0308800, and 2022YFA1403400), Shanghai Science and Technology Plan (21DZ2260400), and Beijing Natural Science Foundation (Z190010, Z210006, and Z190006). We thank the support from the Analytical Instrumentation Center (# SPST-AIC10112914), School of Physical Science and Technology (SPST), ShanghaiTech University, and the staffs from BL15U1 at Shanghai Synchrotron Radiation Facility for assistance during data collection. We also thank Prof. Yanming Ma for the valuable discussion.

  

**Author contributions** Pei C and Qi Y carried out the project and wrote the original draft; Zhu P and Wang Z synthesized and characterized the samples; Zhang Q, Ying T, and Gu L performed the TEM studies; Pei C, Zhao Y, Gao L, Li C, Zhu S, Gao B, Gou H, and Qi Y performed the high-pressure experiments; Li B, Yao YS, Sun J, and Liu H carried out the theoretical calculations; Wang Z and Qi Y supervised the project; Chen Y and Yao YG contributed to the discussion. All authors contributed to the general discussion.

**Conflict of interest** The authors declare that they have no conflict of interest.

**Supplementary information** Supporting data are available in the online version of the paper.

**Cuiying Pei** is a research assistant professor at the School of Physical Science and Technology, ShanghaiTech University. She obtained her PhD degree from Jilin University in 2014. Her current research interests are exploring novel quantum properties under high pressures.

**Peng Zhu** is currently a PhD student at Beijing Institute of Technology (BIT) supervised by Professor Zhiwei Wang. He obtained his Master's degree from BIT in 2021. His research interests are in the fields of single crystal growth, characterization and physical properties of topological materials, especially in bulk-insulating topological insulators.

**Zhiwei Wang** is currently a professor at the School of Physics, BIT. He obtained his PhD degree from the Institute of Physics, Chinese Academy of Sciences in 2012. His research interests are single crystal growth, and physical properties of quantum materials, including topological materials, Kagome lattice, unconventional superconductors, and two-dimensional (2D) materials.

**Yanpeng Qi** is an assistant professor at the School of Physical Science and Technology, ShanghaiTech University. He obtained his PhD degree from the Institute of Electrical Engineering, Chinese Academy of Sciences in 2011. His current research interest focuses on the understanding of novel properties of quantum materials under high pressures, and the design and synthesis of new superconductors.

## 拓扑异质结$(PbSe)_5(Bi_2Se_3)_6$高压诱导超导电性研究

裴翠颖[1†], 朱鹏[2,3,4†], 李炳谈[5,6], 赵毅[1], 高玲玲[1], 李昌华[1], 朱世豪[1], 张庆华[7], 应天平[7], 谷林[7], 高波[8], 缑慧阳[8], 姚延荪[9], 孙建[10], 刘寒雨[5,6], 陈宇林[1,11,12], 王秩伟[2,3,4*], 姚裕贵[2,3], 齐彦鹏[1,11,13*]

**摘要** 最近, 天然异质结$(PbSe)_5(Bi_2Se_3)_6$在理论上预测并实验证实为拓扑绝缘体. 本文通过高压原位量子调控在$(PbSe)_5(Bi_2Se_3)_6$中成功引入超导电性. 当压力增加到10 GPa时, 超导电性突然出现, $T_c$约为4.6 K, 随后$T_c$急剧下降. 值得注意的是, 当进一步施加压力到30 GPa以上时, 出现了一种新的超导态, 且$T_c$直到本实验最高压力仍未饱和. 结合XRD和拉曼光谱, 我们认为$(PbSe)_5(Bi_2Se_3)_6$中两个超导态的出现与压力诱导的结构相变有关. 拓扑异质结压力下出现新的量子态, 为进一步研究拓扑和超导的关系提供了一个良好的平台.

  